Table V. Crystallographic Data for $[Co_2\{(Me_2(NH)_2mxyl)_2([16]cyclidene)_2\}]Cl_4 \cdot 2CH_3OH$

formula	$Co_2C_{52}H_{64}N_{12}Cl_4 \cdot 2CH_3OH$
fw	1180.95
cell params	
a, Å	11.121 (1)
b, Å	13.738 (3)
c, Å	20.185 (2)
α, deg	90
β, deg	99.15 (1)
γ, deg	90
V, Å^3	3044.6
Z	2
space group	$P2_1/c$
F_{000}	1202.0
D_{calcd}, g cm^{-3}	1.287
D_{obsd}, g cm^{-3}; method	1.30 (1); flotation in CCl_4/heptane
radiation	Mo Kα
2θ range, deg	$4 \le 2\theta \le 44$
no. of obsd reflcns ($I \ge 3\sigma(I)$)	1623
no. of params	164
final R factor	
R	0.070
R_w	0.080
goodness of fit (GOF)	4.426

of scattering power of the crystal. The data were corrected for background and Lorentz and polarization effects. Programs XRAY-70 and CRYM were used. The Wilson method was used to bring F^2 to a relatively absolute scale. The I^2 were scaled by increasing the I^2 obtained from counting statistics by PI^2, where P was chosen as the rms deviation of the standard reflections. Scattering factors were taken from the literature.[21,22]

The structure was solved by conventional heavy-atom methods. The positions of the remaining non-hydrogen atoms were revealed by subsequent Fourier syntheses. Refinement was performed by using full-matrix least-squares techniques during which the function $\sum(w(|F_o| - |F_c|))^2$ was minimized. The data were weighted according to $1/(\sigma_F)^2$. Residuals were calculated as $R = \sum||F_o| - |F_c||/\sum|F_o|$, and $R_w = (\sum w(|F_o| - |F_c|)^2/\sum w|F_o|^2)^{1/2}$. Isotropic refinement converged at $R = 0.073$. At this point, the thermal parameters of the cobalt and chlorine were allowed to vary anisotropically. The remaining atoms were constrained to be isotropic scatterers owing to the limited size of the data set. Subsequent full-matrix least-squares refinement converged to the herewith reported determination with $R = 0.070$ and $R_w = 0.080$. In the final cycle of refinement, no atom shifted more than 0.08 of any associated esd. A final difference Fourier map was featureless.

Acknowledgment. We wish to thank Dr. Thomas J. Meade for his assistance in magnetic susceptibility measurements. We are also grateful to Dr. J. Gallucci for the collection of X-ray diffraction data. The support of the National Institutes of Health is gratefully acknowledged.

Supplementary Material Available: A complete listing of observed and calculated structure factors (25 pages). Ordering information is given on any current masthead page.

---

(21) Stewart, R. F.; Davidson, E. R.; Simpson, W. T. *J. Chem. Phys.* **1965**, *42*, 3175–3187.

(22) (a) Cromer, D. T.; Mann, J. B. *Acta Crystallogr., Sect. A: Cryst. Phys., Diffr., Theor. Gen. Crystallogr.* **1968**, *A24*, 321–324. (b) *International Tables for X-Ray Crystallography*; Ibers, J. A., Hamilton, W. C., Eds.; Kynoch: Birmingham, England, 1974; Vol. 1, pp 149–150.

Contribution from the Departments of Chemistry, The University of North Carolina,
Chapel Hill, North Carolina 27514, and The University of Wyoming, Laramie, Wyoming 82071

Barium Binding to γ-Carboxyglutamate and β-Carboxyaspartate Residues: Structures of Barium Complexes of Benzylmalonate, Dimethylmalonate, and Ethylmalonate Ions

Yoshinobu Yokomori,[1a,b] Kathleen A. Flaherty,[1a] and Derek J. Hodgson*[,1c]

Received October 14, 1987

The molecular structures of four barium complexes of substituted malonate ions have been determined from X-ray diffraction data. The 1:2 benzylmalonate complex $Ba(bzmalH)_2 \cdot H_2O$, $Ba(C_{10}O_4H_9)_2 \cdot H_2O$, crystallizes in the orthorhombic space group $Cmc2_1$ with four molecules in a cell of dimensions $a = 34.085$ (13) Å, $b = 7.153$ (2) Å, and $c = 9.024$ (5) Å, and its structure has been refined to a final R factor of 0.050. The 1:1 complex $Ba(bzmal) \cdot 3H_2O$, $BaC_{10}O_4H_8 \cdot 3H_2O$, crystallizes in the monoclinic space group $P2_1/c$ with four molecules in a cell of dimensions $a = 14.373$ (3) Å, $b = 5.489$ (4) Å, $c = 16.892$ (3) Å, and $\beta = 111.4$ (1)°, and its structure has been refined to an R factor of 0.074. The 1:1 dimethylmalonate complex $[Ba(dmal)]_2 \cdot 5H_2O$, $Ba_2(C_5O_4H_6)_2 \cdot 5H_2O$, crystallizes in the monoclinic space group $P2_1/n$ with four molecules in a cell of dimensions $a = 6.194$ (7) Å, $b = 22.010$ (16) Å, $c = 13.225$ (7) Å, and $\beta = 95.62$ (5)°, and its structure has been refined to an R factor of 0.060. The 1:2 ethylmalonate complex $Ba(emalH)_2 \cdot H_2O$, $BaC_{10}O_8H_{14} \cdot H_2O$, is orthorhombic, of space group $Pnma$, with four molecules in a cell of dimensions $a = 10.829$ (2) Å, $b = 26.542$ (10) Å, and $c = 4.760$ (8) Å and has been refined to an R factor of 0.034. All four complexes are polymeric, revealing all three of the possible modes of binding of a metal ion to a dicarboxylate moiety. The significance of these structural features in determining the binding strengths of normal and abnormal prothrombin in barium salts is discussed, as is the distinction between the binding of magnesium and beryllium on the one hand and calcium and barium on the other.

The existence and biological significance of both γ-carboxygutamic (Gla) and β-carboxyaspartic (Asa) acid residues in numerous proteins are well documented,[2-8] although the precise reason(s) for these posttranslational carboxylations is not completely understood. It is, however, well established that Gla residues are implicated in calcium binding,[9] although an equally important function may be to provide sites for interactions with neighboring arginine (Arg) residues, thereby bringing about conformational changes necessary for protein function.[10] It is also known that calcium ions, while binding to the Gla residues,

---

(1) (a) The University of North Carolina. (b) Permanent address: Department of Chemistry, The National Defense Academy, Hashirimizu, Yokosuka 239, Japan. (c) The University of Wyoming.

(2) Magnusson, S.; Sottrup-Jensen, L.; Peterson, T. E.; Morris, H. R.; Dell, A. *FEBS Lett.* **1974**, *44*, 189–193.

(3) Stenflo, J.; Fernlund, P.; Egan, W.; Roepstorff, P. *Proc. Natl. Acad. Sci. U.S.A.* **1974**, *71*, 2730–2733.

(4) Prendergast, F. G.; Mann, K. G. *J. Biol. Chem.* **1977**, *252*, 840–850.

(5) Suttie, J. W.; Jackson, C. M. *Physiol. Rev.* **1977**, *57*, 1–70.

(6) Lian, J. B.; Hauschka, P. V.; Gallop, P. M. *Fed. Proc., Fed. Am. Soc. Exp. Biol.* **1978**, *37*, 2615–2620.

(7) Christy, M. R.; Barkley, R. M.; Koch, T. H.; Van Buskirk, J. J.; Kirsch, W. M. *J. Am. Chem. Soc.* **1981**, *103*, 3935–3937.

(8) Christy, M. R.; Koch, T. H. *J. Am. Chem. Soc.* **1982**, *104*, 1771–1772.

(9) Jackson, C. M.; Nemerson, Y. *Annu. Rev. Biochem.* **1980**, *49*, 765–811.

(10) Craig, D. H.; Koehler, K. A.; Hiskey, R. G. *J. Org. Chem.* **1983**, *48*, 3954–3960.

0020-1669/88/1327-2300$01.50/0

protect the Gla from decarboxylation;[11] a similar rôle for Arg has been suggested, and two reasonable structural models have been proposed.[12,13]

Several authors have suggested that a principal rôle for Gla is in the discrimination between calcium and magnesium,[14] and we and others[15-18] have examined model complexes designed to probe the modes of binding of calcium and magnesium to Gla and/or Asa. The modes of binding of metals to carboxylate groups have been examined in detail by Einspahr and Bugg,[19] who report that a dicarboxylate moiety like that in the side chains of Asa and Gla can bind to a metal (e.g. calcium) in three distinct ways, all of which are shown in **1**. The binding mode involving M(1) is unidentate, while that involving M(2) is bidentate; the mode involving M(3) is sometimes referred to as the "malonate mode" because it is available only to a dicarboxylate (like malonate, Gla, or Asa) and unavailable to a monocarboxylate (like Glu and Asp).

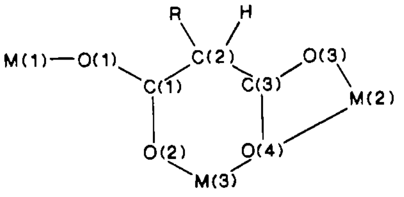

1

Relatively less is known about the binding of these important residues to barium and to other group II (alkaline-earth) metals. Early workers noted that abnormal prothrombin, in which the Gla residues are replaced by Glu, does not adsorb onto barium citrate, and this is used as a means of separating normal and abnormal prothrombin,[20-22] but while this was presumably related to the same sites as are involved in calcium binding,[20] there were no data to suggest that the modes of binding of calcium and barium were similar.

Both high- and low-resolution crystal structures of prothrombin fragment 1, which contains 10 Gla residues, have appeared, but the extensive disorder found in the metal-binding region of the zymogen does not allow for the resolution of the Gla residues. Consequently, since no definitive crystallographic study of a metal complex of Gla or Asa has appeared, the modes of binding of metals to these species are best probed by the use of suitable models. All three binding modes depicted in **1** are available to substituted malonate ions, which suggests that these ions may be suitable models. Metal complexes of the malonate ion itself have been extensively studied,[23-28] but no structural study of a barium malonate complex is available. Moreover, the lack of a substituent at C(2) in the malonate ion renders it a less attractive model for Gla and/or Asa than the α-alkylmalonates. The nature of the binding of calcium to α-ethylmalonate, α-benzylmalonate, and α-methylmalonate has been reported,[15,17,18] as has the interaction between magnesium and α-methylmalonate.[15] We here report the structures of barium complexes of hydrogen α-benzylmalonate {[Ba(bzmalH)$_2$]·H$_2$O}, α-benzylmalonate {[Ba(bzmal)]·3H$_2$O}, α,α-dimethylmalonate {[Ba(dmal)]$_2$·5H$_2$O}, and hydrogen α-ethylmalonate {[Ba(emalH)$_2$]·H$_2$O} ions.

Table I. Crystal and Intensity Measurement Data

	Ba(bzmalH)$_2$·H$_2$O	Ba(bzmal)·3H$_2$O
formula	Ba(C$_{10}$O$_4$H$_9$)$_2$·H$_2$O	BaC$_{10}$O$_4$H$_8$·3H$_2$O
mol wt	541.7	383.6
dimens, mm	0.47 × 0.07 × 0.40	0.13 × 0.19 × 0.37
D(calcd), g cm^{-3}	1.635	2.054
D(obsd), g cm^{-3}	1.631 (10)	1.98 (3)
cell constants		
a, Å	34.085 (13)	14.373 (3)
b, Å	7.153 (2)	5.489 (4)
c, Å	9.024 (5)	16.892 (3)
α, deg	90	90
β, deg	90	111.4 (1)
γ, deg	90	90
vol, Å^3	2200 (3)	1241 (2)
Z	4	4
F(000)	1072	744
μ(Mo Kα), cm^{-1}	19.1	33.2
space group	$Cmc2_1$	$P2_1/c$
data collcd	$+h,-k,+l$	$\pm h,+k,+l$
no. of data collcd	1665	1780
no. of data used	723 $I > 3\sigma(I)$	1488 $I > \sigma(I)$
no. of variables	138	163
R	0.050	0.074
R_w	0.060	0.086
Δ/σ	0.26	0.10
S (GOF)	5.68	4.89
	[Ba(dmal)]$_2$·5H$_2$O	Ba(emalH)$_2$·H$_2$O
formula	Ba$_2$(C$_5$O$_4$H$_6$)$_2$·5H$_2$O	BaC$_{10}$O$_8$H$_{14}$·H$_2$O
mol wt	624.96	417.57
dimens, mm	0.47 × 0.37 × 0.10	0.11 × 0.19 × 0.33
D(calcd), g cm^{-3}	2.313	2.018
D(obsd), g cm^{-3}	2.26 (2)	1.99 (2)
cell constants		
a, Å	6.194 (7)	10.829 (2)
b, Å	22.010 (16)	26.542 (10)
c, Å	13.225 (7)	4.760 (8)
α, deg	90	90
β, deg	95.62 (5)	90
γ, deg	90	90
vol, Å^3	1794 (5)	1368 (3)
Z	4	4
F(000)	1192	808
μ(Mo Kα), cm^{-1}	45.6	30.35
space group	$P2_1/n$	$Pnma$
data collcd	$+h,+k,\pm l$	$+h,+k,+l$
no. of data collcd	3558	1033
no. of data used	2022 $I > 2\sigma(I)$	731 $I > 3\sigma(I)$
no. of variables	216	94
R	0.060	0.034
R_w	0.060	0.045
Δ/σ	0.26	0.04
S (GOF)	1.71	2.89

Experimental Section

Synthesis. All complexes were synthesized by means of approximately the same general technique. Barium hydroxide was added to an aqueous solution containing a 10-fold excess of the appropriate substituted malonic acid, and the resulting mixture was stirred and allowed to sit until crystals formed. Use of a stoichiometric mixture proved unsuccessful in all cases, but use of a slight excess of benzylmalonic acid did allow the

---

(11) Bajaj, S. P.; Price, P. A.; Russell, W. A. *J. Biol. Chem.* **1982**, *257*, 3726–3731.

(12) Gray, A. L.; Hoke, R. A.; Deerfield, D. W., II; Hiskey, R. G. *J. Org. Chem.* **1985**, *50*, 2189–2191.

(13) Yokomori, Y.; Hodgson, D. J. *Int. J. Pept. Protein Res.* **1988**, *31*, 289–298.

(14) Williams, R. J. P. In *Calcium Binding Proteins and Calcium Function*; Wasserman, R. H., et al., Eds.; Elsevier: New York, 1977; pp 1–12.

(15) Curry, M. E.; Eggleston, D. S.; Hodgson, D. J. *J. Am. Chem. Soc.* **1985**, *107*, 8234–8238.

(16) Eggleston, D. S., private communication.

(17) Yokomori, Y.; Hodgson, D. J. *Inorg. Chem.*, in press.

(18) Zell, A.; Einspahr, H.; Bugg, C. E. *Biochemistry* **1985**, *24*, 533–537.

(19) Einspahr, H.; Bugg, C. E. *Acta Crystallogr., Sect. B: Struct. Crystallogr. Cryst. Chem.* **1981**, *B37*, 1044–1052.

(20) Nelsestuen, G. L.; Suttie, J. W. *Biochemistry* **1972**, *11*, 4961–4964.

(21) Stenflo, J.; Ganrot, P. O. *J. Biol. Chem.* **1972**, *247*, 8160–8166.

(22) Nelsestuen, G. L.; Suttie, J. W. *J. Biol. Chem.* **1972**, *247*, 8176–8182.

(23) Briggman, B.; Oskarsson, A. *Acta Crystallogr., Sect. B: Struct. Crystallogr. Cryst. Chem.* **1977**, *B33*, 1900–1906.

(24) Karipides, A.; Ault, J.; Reed, A. T. *Inorg. Chem.* **1977**, *16*, 3299–3302 and references therein. Marsh, R. E.; Schomaker, V. *Inorg. Chem.* **1979**, *18*, 2331–2336.

(25) Albertsson, J.; Oskarsson, A.; Svensson, C. *Acta Crystallogr., Sect. B: Struct. Crystallogr. Cryst. Chem.* **1978**, *B34*, 2737–2743.

(26) Briggman, B.; Oskarsson, A. *Acta Crystallogr., Sect. B: Struct. Crystallogr. Cryst. Chem.* **1978**, *B34*, 3357–3359.

(27) Soriano-Garcia, M.; Rao, S. N. *Acta Crystallogr., Sect. C: Cryst. Struct. Commun.* **1983**, *C39*, 850–852.

(28) Duc, G.; Faure, R.; Loiseleur, H. *Acta Crystallogr., Sect. B: Struct. Crystallogr. Cryst. Chem.* **1978**, *B34*, 2115–2118.

Table II. Atomic Positional Parameters for Ba(bzmalH)$_2$·H$_2$O

atom	x	y	z
Ba	0.0000	0.06219 (8)	0.7558
O(1)	0.0945 (3)	0.5678 (7)	0.8788 (13)
O(2)	0.0539 (2)	0.3602 (11)	0.7936 (12)
O(3)	0.0637 (2)	0.1982 (8)	1.2088 (8)
O(4)	0.0460 (3)	0.0474 (10)	1.0048 (14)
OW(1)	0.0000	0.3033 (14)	0.4841 (27)
C(1)	0.0802 (3)	0.400 (1)	0.875 (1)
C(2)	0.0985 (3)	0.266 (1)	0.984 (1)
C(3)	0.0665 (3)	0.166 (1)	1.073 (1)
C(4)	0.1230 (3)	0.121 (2)	0.898 (2)
C(5)	0.1576 (3)	0.205 (1)	0.814 (1)
C(6)	0.1524 (3)	0.273 (1)	0.670 (2)
C(7)	0.1836 (4)	0.354 (2)	0.595 (2)
C(8)	0.2187 (4)	0.369 (2)	0.662 (2)
C(9)	0.2250 (3)	0.301 (2)	0.805 (2)
C(10)	0.1943 (3)	0.220 (2)	0.882 (2)

Table III. Atomic Positional Parameters for Ba(bzmal)·3H$_2$O

atom	x	y	z
Ba	0.48541 (6)	0.1777 (2)	0.12953 (5)
O(1)	0.3947 (8)	0.343 (2)	0.4478 (6)
O(2)	0.3850 (7)	−0.058 (2)	0.4252 (6)
O(3)	0.3908 (7)	0.387 (2)	0.2407 (6)
O(4)	0.3864 (7)	−0.021 (2)	0.2419 (6)
OW(1)	0.4212 (7)	0.682 (2)	0.0865 (6)
OW(2)	0.2359 (8)	0.706 (2)	0.1150 (7)
OW(3)	0.2579 (9)	0.215 (2)	0.0572 (7)
C(1)	0.363 (1)	0.159 (3)	0.4040 (9)
C(2)	0.292 (1)	0.197 (3)	0.3109 (9)
C(3)	0.361 (1)	0.186 (3)	0.2600 (8)
C(4)	0.231 (1)	0.432 (4)	0.2941 (11)
C(5)	0.153 (1)	0.446 (4)	0.3363 (11)
C(6)	0.078 (1)	0.259 (4)	0.3211 (11)
C(7)	0.006 (1)	0.281 (5)	0.3550 (12)
C(8)	0.008 (1)	0.508 (6)	0.4022 (12)
C(9)	0.080 (1)	0.690 (4)	0.4187 (11)
C(10)	0.151 (1)	0.658 (4)	0.3850 (11)

formation of the 1:1 complex Ba(bzmal)·3H$_2$O. All complexes gave satisfactory analyses. No attempt was made to maximize the yields, since we were interested in obtaining good crystals; actual yields were less than 20% (based on added barium) in each case. All crystals were obtained as very small needles, with maximum lengths of less than 0.4 mm and thicknesses of 0.1 mm.

X-ray Data Collection and Reduction. Cell constants for each crystal were obtained at 293 K from least-squares analysis of the angular settings of 25 reflections with $8 < \theta(\mathrm{Mo}) < 15°$ [Ba(bzmalH)$_2$], $8 < \theta(\mathrm{Mo}) < 15°$ [Ba(bzmal)], $8 < \theta(\mathrm{Mo}) < 17°$ [Ba(dmal)], and $8 < \theta(\mathrm{Mo}) < 16°$ [Ba(emalH)$_2$] on an Enraf-Nonius CAD-4 diffractometer with molybdenum radiation and Zr filter [($\lambda_{\mathrm{Mo}\,K\alpha}$) = 0.71073 Å]. Intensity data were corrected for Lorentz-polarization effects; since the crystals were very small, no absorption corrections were applied. The maximum effect of absorption, as estimated from ψ-scan data for the emalH crystal, was less than 5% on I. Orientation and intensity standards were monitored after every 200 reflections and 3 h of exposure time, respectively. No corrections for decay were necessary. All least-squares refinements were full matrix, the weighting scheme used being that of Ibers and coworkers[29] with $p = 0.02$. Additional crystallographic information is presented in Table I.

Each structure was solved by direct methods using MULTAN80. Nonhydrogen atoms were refined with anisotropic temperature factors. Hydrogen atoms were placed in fixed calculated positions with C–H = 0.95 and O–H = 0.90 Å and assigned fixed isotropic temperature factors (5.0 Å^2); hydrogen atom parameters were not refined. Neutral-atom scattering factors were used for non-hydrogen atoms and were taken from ref 30; hydrogen atom scattering factors were those of Stewart et al.[31] Anomalous dispersion corrections were from ref 30. Final atomic positional parameters for the four crystal structures, along with their standard

Table IV. Atomic Positional Parameters for [Ba(dmal)]$_2$·5H$_2$O

atom	x	y	z
Ba(1)	0.1030 (2)	0.26120 (5)	0.23741 (9)
Ba(2)	0.1359 (2)	0.12681 (5)	−0.11373 (9)
O(1)	−0.172 (2)	0.2533 (6)	0.3889 (9)
O(2)	−0.270 (2)	0.2702 (7)	0.5417 (9)
O(3)	−0.020 (2)	0.1758 (6)	0.7042 (9)
O(4)	0.234 (2)	0.2193 (6)	0.6171 (11)
O(11)	0.256 (2)	0.4410 (6)	0.3408 (11)
O(12)	−0.003 (2)	0.3797 (6)	0.2724 (9)
O(13)	−0.230 (2)	0.4951 (6)	0.3576 (10)
O(14)	−0.092 (2)	0.5796 (6)	0.3013 (10)
OW(1)	0.294 (2)	0.2982 (6)	0.4403 (10)
OW(2)	0.072 (2)	0.0538 (6)	0.0643 (9)
OW(3)	0.455 (2)	0.1871 (6)	0.2882 (10)
OW(4)	0.459 (2)	0.3509 (6)	0.6833 (11)
OW(5)	0.028 (2)	0.3890 (6)	0.5026 (11)
C(2)	−0.079 (3)	0.1804 (9)	0.520 (1)
C(3)	0.053 (3)	0.1920 (8)	0.623 (1)
C(4)	−0.255 (3)	0.1345 (9)	0.532 (1)
C(5)	0.067 (4)	0.1491 (9)	0.447 (1)
C(11)	0.086 (3)	0.4297 (9)	0.281 (1)
C(13)	−0.119 (3)	0.5231 (8)	0.299 (1)
C(14)	0.169 (3)	0.5213 (9)	0.172 (1)
C(15)	−0.181 (3)	0.4667 (10)	0.135 (2)
C(1)	−0.181 (3)	0.2396 (9)	0.480 (1)
C(12)	−0.011 (3)	0.4853 (8)	0.219 (1)

Table V. Atomic Positional Parameters for Ba(emalH)$_2$·H$_2$O

atom	x	y	z
Ba	0.62585 (6)	0.2500 (0)	0.6394 (1)
O(1)	0.5737 (5)	0.3102 (2)	1.1355 (9)
O(2)	0.6345 (4)	0.3867 (2)	1.2578 (12)
O(3)	0.2634 (4)	0.3389 (2)	0.8892 (10)
O(4)	0.4253 (5)	0.3182 (2)	0.6384 (10)
O(5)	0.7961 (8)	0.2500 (0)	1.1878 (21)
C(1)	0.5596 (7)	0.3558 (3)	1.131 (1)
C(2)	0.4511 (8)	0.3807 (3)	0.993 (2)
C(3)	0.3750 (6)	0.3425 (3)	0.827 (1)
C(4)	0.4623 (11)	0.4294 (4)	0.881 (2)
C(5)	0.3564 (9)	0.4570 (3)	0.768 (2)

Table VI. Bond Lengths (Å) in Ba(bzmalH)$_2$·H$_2$O[a]

Ba–O(2)	2.835 (4)	C(2)–C(4)	1.540 (8)
Ba–O(3)^4	2.891 (4)	C(3)–O(3)	1.248 (6)
Ba–O(4)	2.741 (5)	C(3)–O(4)	1.262 (7)
Ba–O(4)^4	2.863 (6)	C(4)–C(5)	1.527 (8)
Ba–OW(1)	2.997 (9)	C(5)–C(6)	1.401 (8)
C(1)–O(1)	1.295 (5)	C(5)–C(10)	1.396 (8)
C(1)–O(2)	1.192 (6)	C(6)–C(7)	1.387 (9)
C(1)–C(2)	1.514 (7)	C(7)–C(8)	1.350 (10)
C(2)–C(3)	1.529 (7)	C(8)–C(9)	1.390 (10)
		C(9)–C(10)	1.380 (10)

[a] Symmetry operations are given as superscripts: $4 = x, -y, -\frac{1}{2} + z$.

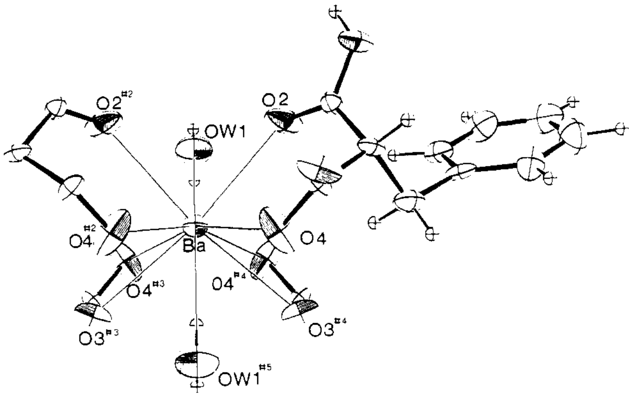

Figure 1. View of the coordination around barium in [Ba(bzmalH)$_2$]·H$_2$O. In this and some of the following figures, many carbon atoms have been omitted from the figure for clarity.

---

(29) Corfield, P. W. R.; Doedens, R. J.; Ibers, J. A. *Inorg. Chem.* **1967**, *6*, 197–204.

(30) *International Tables for X-ray Crystallography*; Kynoch: Birmingham, England, 1974; Vol. IV.

(31) Stewart, R. F.; Davidson, E. R.; Simpson, W. T. *J. Chem. Phys.* **1965**, *42*, 3175–3187.

Table VII. Bond Angles (deg) in $Ba(bzmalH)_2 \cdot H_2O^a$

$O(2)-Ba-O(2)^2$	80.8 (2)	$O(2)-Ba-O(3)^3$	171.4 (1)
$O(2)-Ba-O(3)^4$	90.9 (1)	$O(2)-Ba-O(4)$	63.9 (1)
$O(2)-Ba-O(4)^2$	107.5 (2)	$O(2)-Ba-O(4)^3$	131.0 (2)
$O(2)-Ba-O(4)^4$	86.9 (2)	$O(2)-Ba-OW(1)$	70.5 (2)
$O(2)-Ba-OW(1)^5$	121.1 (1)	$O(3)^3-Ba-O(3)^4$	97.3 (2)
$O(3)^3-Ba-O(4)$	121.6 (1)	$O(3)^3-Ba-O(4)^2$	70.5 (2)
$O(3)^3-Ba-O(4)^3$	45.3 (1)	$O(3)^3-Ba-O(4)^4$	96.8 (1)
$O(3)^3-Ba-OW(1)$	104.5 (1)	$O(3)^3-Ba-OW(1)^5$	65.5 (1)
$O(4)-Ba-O(4)^2$	69.7 (3)	$O(4)-Ba-O(4)^3$	161.9 (0)
$O(4)-Ba-O(4)^4$	109.0 (2)	$O(4)-Ba-OW(1)$	133.8 (1)
$O(4)-Ba-OW(1)^5$	57.5 (2)	$O(4)^3-Ba-O(4)^4$	66.3 (2)
$O(4)^3-Ba-OW(1)$	60.7 (2)	$O(4)^3-Ba-OW(1)^5$	105.9 (2)
$OW(1)-Ba-OW(1)^5$	163.4 (3)		
$O(1)-C(1)-O(2)$	121.5 (5)	$O(1)-C(1)-C(2)$	114.6 (4)
$O(2)-C(1)-C(2)$	123.9 (4)	$C(1)-C(2)-C(3)$	110.2 (4)
$C(1)-C(2)-C(4)$	108.8 (4)	$C(3)-C(2)-C(4)$	109.7 (3)
$O(3)-C(3)-O(4)$	124.1 (5)	$O(3)-C(3)-C(2)$	119.0 (4)
$O(4)-C(3)-C(2)$	116.8 (5)	$C(2)-C(4)-C(5)$	113.9 (4)
$C(4)-C(5)-C(6)$	120.1 (5)	$C(4)-C(5)-C(10)$	120.5 (6)
$C(6)-C(5)-C(10)$	119.3 (6)	$C(5)-C(6)-C(7)$	120.3 (6)
$C(6)-C(7)-C(8)$	119.5 (7)	$C(7)-C(8)-C(9)$	121.6 (7)
$C(8)-C(9)-C(10)$	119.7 (8)	$C(5)-C(10)-C(9)$	119.5 (7)

[a] Symmetry operations as in Table VI, plus the following: $2 = -x, y, z$; $3 = -x, -y, -{}^1/_2 + z$; $5 = -x, -y, {}^1/_2 + z$.

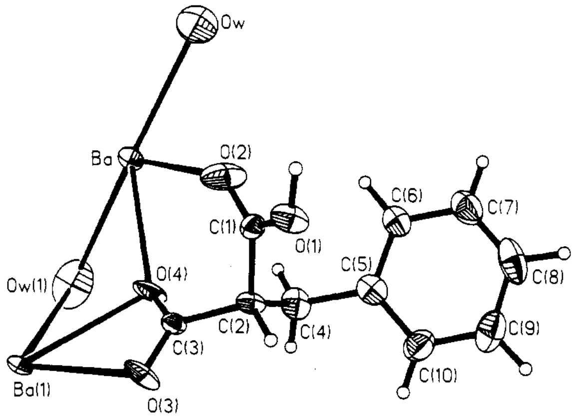

Figure 2. Binding of a single $bzmalH^-$ ion in $Ba(bzmalH)_2 \cdot H_2O$. Atoms labeled Ba(1) and OW(1) are related to the parent atoms by the symmetry operation $-x, -y, {}^1/_2 + z$.

deviations as estimated from the inverse least-squares matrix, are presented in Tables II–V.

Description of Structures

$[Ba(bzmalH)_2] \cdot H_2O$. The structure consists of Ba^{2+} cations coordinated to two $bzmalH^-$ anions and water molecules. As is invariably the case for calcium complexes of malonate derivatives, the structure is polymeric, each unit being linked by anions and by water molecules. The barium atom sits on a crystallographic mirror plane, as does the water molecule; a view of the coordination environment around the barium atom is depicted in Figure 1. Bond lengths and angles in the complex are available in Tables VI and VII, respectively.

As can be seen in Figure 1, the coordination polyhedron around barium is 10-coordinate. Ba exhibits two of the three possible (vide supra) binding modes to the $bzmalH^-$ ions shown in **1**: the bidentate coordination through O(3) and O(4) and the malonate coordination through O(2) and O(4). Additionally, each barium center is coordinated to two symmetry-related water molecules, OW(1) and OW(1)′.

The Ba–O(malonate) distances are in the range 2.741 (5)–2.891 (9) Å, which is consistent with values reported for other barium carboxylate structures.[32,33] The C(1)–C(2)–C(3) bond angle of 110.2° at C(2) is normal, suggesting that the six-membered ring is relatively free from internal strain; significant deviations from tetrahedral geometry have been observed in some metal malonate complexes that exhibit the malonate coordination mode.[26-28]

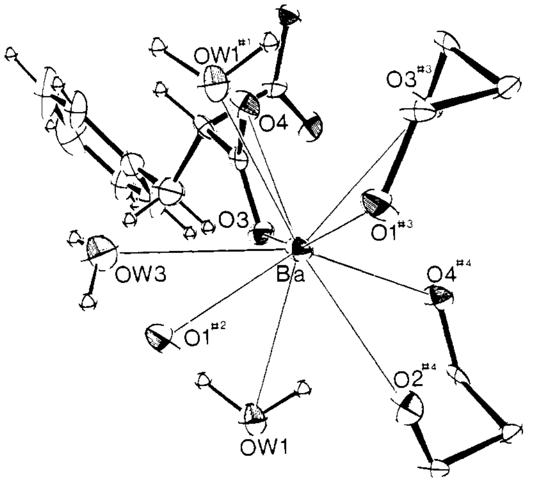

Figure 3. View of the coordination around barium in $[Ba(bzmal)] \cdot 3H_2O$.

Table VIII. Bond Lengths (Å) in $Ba(bzmal) \cdot 3H_2O^a$

$Ba-O(1)^2$	2.866 (5)	$Ba-O(1)^3$	3.113 (5)
$Ba-O(2)^4$	2.773 (5)	$Ba-O(3)$	2.925 (5)
$Ba-O(3)^3$	2.770 (5)	$Ba-O(4)$	2.966 (5)
$Ba-O(4)^4$	2.813 (5)	$Ba-OW(1)^1$	2.878 (5)
$Ba-OW(1)$	2.926 (5)	$Ba-OW(3)$	3.051 (6)
$C(1)-O(1)$	1.236 (8)	$C(1)-O(2)$	1.254 (8)
$C(1)-C(2)$	1.542 (9)	$C(2)-C(3)$	1.530 (9)
$C(2)-C(4)$	1.530 (10)	$C(3)-O(3)$	1.264 (8)
$C(3)-O(4)$	1.267 (8)	$C(4)-C(5)$	1.530 (10)
$C(5)-C(6)$	1.440 (10)	$C(5)-C(10)$	1.430 (10)
$C(6)-C(7)$	1.360 (10)	$C(7)-C(8)$	1.470 (10)
$C(8)-C(9)$	1.400 (10)	$C(9)-C(10)$	1.360 (10)

[a] Symmetry operations are given as superscripts: $1 = x, -1 + y, z$; $2 = x, {}^1/_2 - y, -{}^1/_2 + z$; $3 = 1 - x, -{}^1/_2 + y, {}^1/_2 - z$; $4 = 1 - x, {}^1/_2 + y, {}^1/_2 - z$.

A view of the binding of a single $bzmalH^-$ ion is shown in Figure 2. As can be seen, each malonate is coordinated to only two different barium cations. The polymeric nature of the complex is readily discernible from Figure 2; the structure consists of chains of barium ions that are linked by $bzmalH^-$ ions and by water molecules. The geometry of the hydrogen benzylmalonate ion can be compared with that of free benzylmalonic acid[34] and with that found for the same ion in methylguanidinium hydrogen benzylmalonate.[13] As anticipated, the C–O bond lengths in the two carboxyl groups are different. The geometry of the deprotonated group at C(3) is symmetric, with C(3)–O(3) and C(3)–O(4) distances of 1.248 (6) and 1.262 (7) Å, which are comparable to those of 1.244 (1) and 1.267 (1) Å in the methylguanidinium salt.[13] At the protonated group on C(1), however, there is (formally) one single and one double bond, with C(1)–O(2) and C(1)–O(1) lengths of 1.192 (6) and 1.295 (5) Å, respectively, analogous to the values of 1.196 (4) and 1.316 (5) Å in the free acid[34] and those of 1.208 (1) and 1.318 (1) Å at the protonated site in the methylguanidinium salt.[13] As is observed in other alkylmalonate structures, the two carboxyl groups are non-coplanar. In the present case, the dihedral angle between the planes O(1)–C(1)–O(2) and O(3)–C(3)–O(4) is 60°, the group at C(1) being 50° out of the central-atom plane [C(1)–C(2)–C(3)] while the other group forms an angle of 69° with this plane.

$[Ba(bzmal)] \cdot 3H_2O$. The structure is again polymeric, consisting of Ba^{2+} cations, $bzmal^{2-}$ anions, and water molecules. The geometry around the barium is depicted in Figure 3. The coordination polyhedron is again 10-coordinate, but here all three modes of coordination are found. There are one example of

---

(32) Voegel, J. C.; Thierry, J. C.; Weiss, R. *Acta Crystallogr., Sect. B: Struct. Crystallogr. Cryst. Chem.* **1974**, *B30*, 70–75.

(33) Burns, J. H.; Musikas, C. *Inorg. Chem.* **1977**, *16*, 1619–1622.

(34) Lepore, U.; Lepore, G. C.; Ganis, P. *Acta Crystallogr., Sect. B: Struct. Crystallogr. Cryst. Chem.* **1975**, *B31*, 2874–2876.

Table IX. Bond Angles (deg) in Ba(bzmal)·3H_2O

O(1)^2-Ba-O(1)^3	68.4 (2)	O(1)^2-Ba-O(2)^4	76.2 (1)
O(1)^2-Ba-O(3)	124.6 (1)	O(1)^2-Ba-O(3)^3	137.2 (2)
O(1)^2-Ba-O(4)	122.3 (1)	O(1)^2-Ba-O(4)^4	139.8 (2)
O(1)^2-Ba-OW(1)^1	73.3 (1)	O(1)^2-Ba-OW(1)	78.1 (1)
O(1)^2-Ba-OW(3)	64.7 (1)	O(1)^3-Ba-O(2)^4	68.0 (1)
O(1)^3-Ba-O(3)	163.6 (1)	O(1)^3-Ba-O(3)^3	72.4 (1)
O(1)^3-Ba-O(4)	121.3 (1)	O(1)^3-Ba-O(4)^4	111.3 (1)
O(1)^3-Ba-OW(1)^1	60.9 (1)	O(1)^3-Ba-OW(2)	128.8 (1)
O(1)^3-Ba-OW(3)	123.3 (1)	O(2)^4-Ba-O(3)	122.4 (1)
O(2)^4-Ba-O(3)^3	104.5 (1)	O(2)^4-Ba-O(4)	160.8 (1)
O(2)^4-Ba-O(4)^4	67.7 (1)	O(2)^4-Ba-OW(1)^1	127.1 (1)
O(2)^4-Ba-OW(1)	67.2 (1)	O(2)^4-Ba-OW(3)	125.7 (2)
O(3)-Ba-O(3)^3	91.9 (1)	O(3)-Ba-O(4)	44.7 (1)
O(3)-Ba-O(4)^4	66.5 (1)	O(3)-Ba-OW(1)^1	110.5 (1)
O(3)-Ba-OW(1)	67.0 (1)	O(3)-Ba-OW(3)	63.2 (1)
O(3)^3-Ba-O(4)	66.5 (1)	O(3)^3-Ba-O(4)^4	71.2 (2)
O(3)^3-Ba-OW(1)^1	73.1 (1)	O(3)^3-Ba-OW(1)	142.7 (1)
O(3)^3-Ba-OW(3)	129.8 (2)	O(4)-Ba-O(4)^4	93.1 (1)
O(4)-Ba-OW(1)	68.2 (1)	O(4)-Ba-OW(1)	109.0 (1)
O(4)-Ba-OW(3)	65.6 (1)	O(4)^4-Ba-OW(1)^1	144.0 (1)
O(4)^4-Ba-OW(1)	72.2 (1)	O(4)^4-Ba-OW(3)	125.0 (2)
OW(1)^1-Ba-OW(1)	142.1 (2)	OW(1)^1-Ba-OW(3)	76.4 (2)
OW(1)-Ba-OW(3)	69.0 (2)		
O(1)-C(1)-O(2)	127.5 (6)	O(1)-C(1)-C(2)	117.5 (6)
O(2)-C(1)-C(2)	115.0 (6)	C(1)-C(2)-C(3)	104.4 (5)
C(1)-C(2)-C(4)	115.0 (6)	C(3)-C(2)-C(4)	112.0 (6)
O(3)-C(3)-C(2)	117.3 (6)	O(4)-C(3)-C(2)	118.0 (6)
O(3)-C(3)-O(4)	124.6 (6)	C(2)-C(4)-C(5)	115.2 (7)
C(4)-C(5)-C(6)	120.5 (8)	C(4)-C(5)-C(10)	118.4 (7)
C(6)-C(5)-C(10)	120.8 (7)	C(5)-C(6)-C(7)	119.8 (9)
C(6)-C(7)-C(8)	116.0 (10)	C(7)-C(8)-C(9)	125.4 (8)
C(8)-C(9)-C(10)	116.3 (9)	C(5)-C(10)-C(9)	121.5 (9)

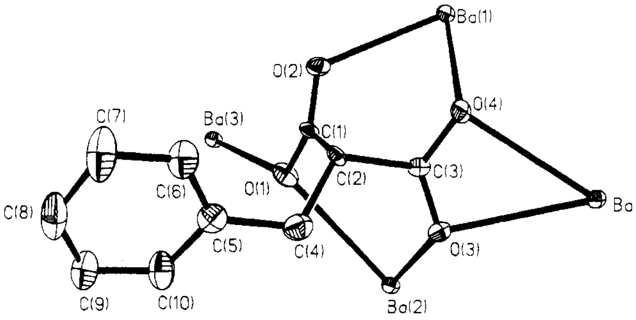

Figure 4. Binding of a single bzmal^{2-} ion in [Ba(bzmal)$_2$]·3H_2O. Atoms labeled Ba(1), Ba(2), and Ba(3) are related to the parent atom by the symmetry operations $1 - x, y - {}^1/_2, {}^1/_2 - z$; $1 - x, {}^1/_2 + y, {}^1/_2 - z$; and $x, {}^1/_2 - y, {}^1/_2 + z$, respectively.

Table X. Bond Lengths (Å) in [Ba(dmal)]$_2$·5H_2O[a]

Ba(1)-O(1)	2.759 (9)	Ba(1)-O(2)^1	2.864 (10)
Ba(1)-O(3)^1	2.786 (9)	Ba(1)-O(4)^2	2.688 (10)
Ba(1)-O(12)	2.741 (10)	Ba(1)-OW(1)	2.940 (10)
Ba(1)-OW(3)	2.753 (10)	Ba(1)-OW(4)	2.697 (11)
Ba(2)-O(1)^1	2.894 (10)	Ba(2)-O(2)^1	3.077 (10)
Ba(2)-O(3)^3	2.728 (10)	Ba(2)-O(11)^2	2.803 (10)
Ba(2)-O(12)^1	2.818 (9)	Ba(2)-O(13)^1	2.845 (10)
Ba(2)-OW(1)^2	2.830 (10)	Ba(2)-OW(2)	2.908 (10)
Ba(2)-OW(5)^1	2.766 (11)		
C(1)-O(1)	1.25 (1)	C(1)-O(2)	1.23 (1)
C(1)-C(2)	1.52 (1)	C(2)-C(3)	1.54 (2)
C(2)-C(4)	1.50 (1)	C(2)-C(5)	1.55 (1)
C(3)-O(3)	1.25 (1)	C(3)-O(4)	1.28 (1)
C(11)-O(11)	1.28 (1)	C(11)-O(12)	1.23 (1)
C(11)-C(12)	1.56 (1)	C(12)-C(13)	1.55 (1)
C(12)-C(14)	1.55 (1)	C(12)-C(15)	1.51 (1)
C(13)-O(13)	1.25 (1)	C(13)-O(14)	1.25 (1)

[a] Symmetry operations are given as superscripts: $1 = {}^1/_2 + x, {}^1/_2 - y, -{}^1/_2 + z$; $2 = -{}^1/_2 + x, {}^1/_2 - y, -{}^1/_2 + z$; $3 = x, y, -1 + z$.

Table XI. Bond Angles (deg) in [Ba(dmal]$_2$·5H_2O

O(1)-Ba(1)-O(2)^1	152.3 (3)	O(1)-Ba(1)-O(3)^1	137.1 (3)
O(1)-Ba(1)-O(4)^2	83.7 (3)	O(1)-Ba(1)-O(12)	76.2 (3)
O(1)-Ba(1)-OW(1)	65.0 (3)	O(1)-Ba(1)-OW(3)	108.4 (3)
O(1)-Ba(1)-OW(4)	85.6 (3)	O(2)^1-Ba(1)-O(3)^1	70.6 (3)
O(2)^1-Ba(1)-O(4)^2	78.3 (3)	O(2)^1-Ba(1)-O(12)	118.3 (3)
O(2)^1-Ba(1)-OW(1)	140.3 (3)	O(2)^1-Ba(1)-OW(3)	78.2 (3)
O(2)^1-Ba(1)-OW(4)^2	69.7 (3)	O(3)^1-Ba(1)-O(4)^2	120.3 (3)
O(3)^1-Ba(1)-O(12)	76.8 (3)	O(3)^1-Ba(1)-OW(1)	74.8 (3)
O(3)^1-Ba(1)-OW(3)	71.2 (3)	O(3)^1-Ba(1)-OW(4)	132.4 (3)
O(4)^2-Ba(1)-O(12)	75.1 (3)	O(4)^2-Ba(1)-OW(1)	137.7 (3)
O(4)^2-Ba(1)-OW(3)	147.8 (3)	O(4)^2-Ba(1)-OW(4)^2	75.4 (3)
O(12)-Ba(1)-OW(1)	70.4 (3)	O(12)-Ba(1)-OW(3)	136.1 (3)
O(12)-Ba(1)-OW(4)^2	146.8 (3)	OW(1)-Ba(1)-OW(3)	72.7 (3)
OW(1)-Ba(1)-OW(4)^2	126.1 (3)	OW(3)-Ba(1)-OW(4)^2	76.0 (3)
O(1)^1-Ba(2)-O(2)^1	43.0 (3)	O(1)^1-Ba(2)-O(3)^3	76.1 (3)
O(1)^1-Ba(2)-O(11)^2	145.5 (3)	O(1)^1-Ba(2)-O(12)^1	72.9 (3)
O(1)^1-Ba(2)-O(13)^1	137.4 (3)		
O(1)^1-Ba(2)-OW(1)^2	77.4 (3)	O(1)^1-Ba(2)-OW(2)	125.6 (3)
O(1)^1-Ba(2)-OW(5)^1	76.7 (3)	O(2)^1-Ba(2)-O(3)^3	109.0 (3)
O(2)^1-Ba(2)-O(11)^2	129.5 (3)	O(2)^1-Ba(2)-O(12)^1	106.6 (3)
O(2)^1-Ba(2)-O(13)^1	138.2 (3)	O(2)^1-Ba(2)-OW(1)^2	60.0 (3)
O(2)^1-Ba(2)-OW(2)	84.2 (3)	O(2)^1-Ba(2)-OW(5)^1	67.8 (3)
O(3)^3-Ba(2)-O(11)^2	78.7 (3)	O(3)^3-Ba(2)-O(12)^1	77.2 (3)
O(3)^3-Ba(2)-O(13)^1	109.8 (3)	O(3)^3-Ba(2)-OW(1)^2	77.5 (3)
O(3)^3-Ba(2)-OW(2)	150.3 (3)	O(3)^3-Ba(2)-OW(5)^1	139.2 (3)
O(11)^2-Ba(2)-O(12)^1	123.5 (3)	O(11)^2-Ba(2)-O(13)^1	73.7 (3)
O(11)^2-Ba(2)-OW(1)^2	74.5 (3)	O(11)^2-Ba(2)-OW(2)	72.7 (3)
O(11)^2-Ba(2)-OW(5)^1	136.5 (3)	O(12)^1-Ba(2)-O(13)^1	67.9 (3)
O(12)^1-Ba(2)-OW(1)^2	144.7 (3)	O(12)^1-Ba(2)-OW(2)	125.6 (3)
O(12)^1-Ba(2)-OW(5)^1	65.9 (3)	O(13)^1-Ba(2)-OW(1)^2	145.0 (3)
O(13)^1-Ba(2)-OW(5)^1	65.9 (3)	O(13)^1-Ba(2)-OW(1)^2	145.0 (3)
O(13)^1-Ba(2)-OW(2)	69.6 (3)	O(13)^1-Ba(2)-OW(5)^1	72.8 (3)
OW(1)^2-Ba(2)-OW(2)	87.4 (3)	OW(1)^2-Ba(2)-OW(5)^1	124.8 (3)
OW(2)-Ba(2)-OW(5)^1	70.2 (3)		
O(1)-C(1)-O(2)	125 (1)	O(1)-C(1)C(2)	119 (1)
O(2)-C(1)-C(2)	115 (1)	C(1)-C(2)-C(3)	109 (1)
C(1)-C(2)-C(4)	109 (1)	C(1)-C(2)-C(5)	114 (1)
C(3)-C(2)-C(4)	110 (1)	C(3)-C(2)-C(5)	109 (1)
C(4)-C(2)-C(5)	103 (1)	O(3)-C(3)-O(4)	125 (1)
O(3)-C(3)-C(2)	120 (1)	O(4)-C(3)-C(2)	114 (1)
O(11)-C(11)-O(12)	124 (1)	O(11)-C(11)-C(12)	115 (1)
O(12)-C(11)-C(12)	120 (1)	C(11)-C(12)-C(13)	103 (1)
C(11)-C(12)-C(14)	110 (1)	C(11)-C(12)-C(15)	112 (1)
C(13)-C(12)-C(14)	111 (1)	C(13)-C(12)-C(15)	109 (1)
C(14)-C(12)-C(15)	109 (1)	O(13)-C(13)-O(14)	123 (1)
O(13)-C(13)-C(12)	117 (1)	O(14)-C(13)-C(12)	119 (1)

unidentate coordination [involving O(1)], one of bidentate coordination [to O(3) and O(4)], and two of the malonate mode; the coordination sphere is completed by three water molecules. Bond lengths and angles in the complex are listed in Tables VIII and IX, respectively.

The Ba-O(malonate) distances of 2.770 (5)-3.113 (5) Å are a little longer than those reported above but are not inconsistent with these or with those in other structures. The bond angle at C(2) [C(1)-C(2)-C(3) = 104.4°] is smaller than the normal value, suggesting that there is greater strain in the present structure than in the bzmalH$^-$ complex above.

The binding of the bzmal^{2-} ions is shown in Figure 4. Each bzmal^{2-} ion binds to four different barium cations. As can be seen in Figure 4, the nature of the polymeric aggregate is entirely different from that in Ba(bzmalH)$_2$. The geometric parameters of the benzylmalonate ion are unremarkable, with symmetric C-O bond lengths at both C(1) and C(3) in the range 1.236 (8)-1.267 (8) Å. One of the carboxyl groups [O(1)-C(1)-O(2)] is 97° out of the plane C(1)-C(2)-C(3) while the other forms an angle with the same plane of 82°; the dihedral angle between the carboxyl groups is 79°.

[Ba(dmal)$_2$]·5H_2O. There are two independent dimethylmalonate dianions, two independent barium cations, and five water molecules in an asymmetric unit. The structure is also polymeric, as were the bzmal complexes. The geometries around the two independent barium atoms, illustrated in Figure 5, are different. The coordination polyhedron at Ba(1) is 8-coordinate while Ba(2) is 9-coordinate. At Ba(1) there are three examples of unidentate coordination, one of malonate coordination, but no bidentate coordination; additionally, there are three coordinated water molecules. At Ba(2) all three coordination modes are observed, with two examples of unidentate coordination, one of bidentate

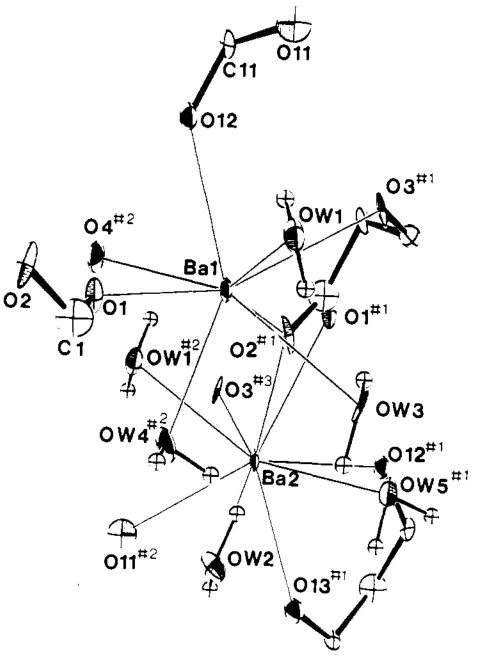

Figure 5. View of the coordination around the two independent barium centers in $[Ba(dmal)]_2 \cdot 5H_2O$.

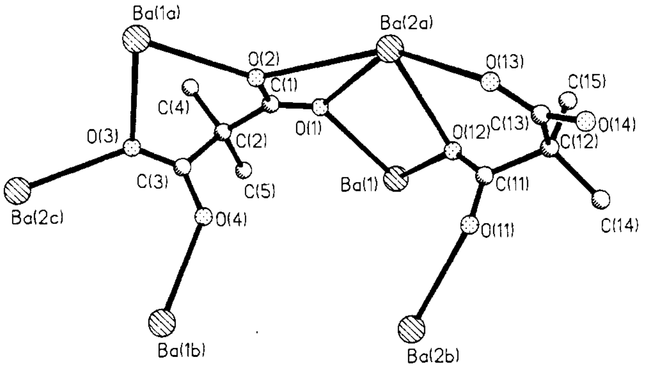

Figure 6. Binding of the two crystallographically independent $dmal^{2-}$ ions in $[Ba(dmal)]_2 \cdot 5H_2O$. Symmetry operations: a = $x - {}^1/_2, {}^1/_2 - y, {}^1/_2 + z$; b = ${}^1/_2 + x, {}^1/_2 - y, {}^1/_2 + z$; c = $x, y, z + 1$.

coordination, and one of malonate coordination in addition to three coordinated water molecules. Bond lengths and angles are listed in Tables X and XI, respectively.

The Ba–O(malonate) distances are in the ranges 2.69 (1)–2.86 (1) Å at Ba(1) and 2.73 (1)–3.08 (1) Å at Ba(2), which are consistent with the other values reported in this paper. The bond angles at the central carbon atoms C(2) [C(1)–C(2)–C(3)] and C(12) [C(11)–C(12)–C(13)] in the two independent dimethylmalonate ions are 109 and 103°, respectively, indicating more strain in the second ion.

The binding of the two independent dimethylmalonate ions to the barium cations is shown in Figure 6. As can be seen in this figure, the polymeric network is formed by a complex set of interactions involving the carboxylate groups of both anions; water molecule OW(1) is also involved in the bridging network. The malonate ion containing oxygen atoms O(1)–O(4) is coordinated to five different barium cations, while the other is coordinated to only three different barium centers. The geometries of the dimethylmalonate ion are normal. One of the carboxyl groups [O(1)–C(1)–O(2)] is rotated by 45° out of the central atom plane [C(1)–C(2)–C(3)] while the other [O(3)–C(3)–O(4)] forms an angle with the same plane of 75°; the dihedral angle between the two carboxyl groups is 87°. In the second ion the corresponding values are 75 and 45° with a dihedral angle between the carboxyl groups of 88°.

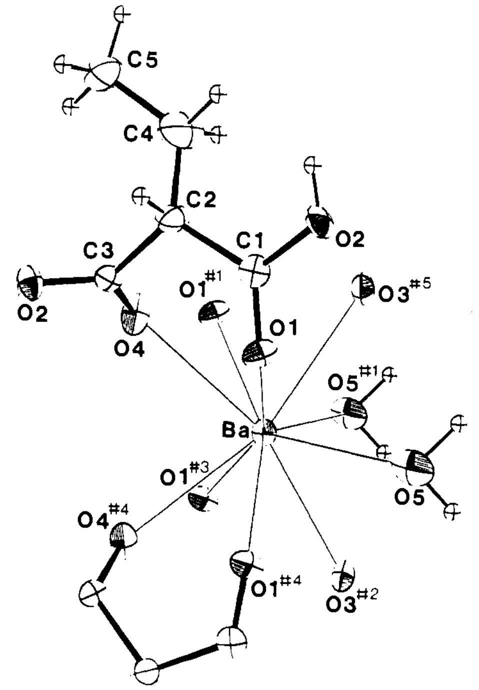

Figure 7. View of the coordination around barium in $[Ba(emalH)_2] \cdot H_2O$.

Table XII. Bond Lengths (Å) in $Ba(emalH)_2 \cdot H_2O^a$

$Ba-O(1)^1$	2.937 (3)	Ba–O(1)	2.907 (3)
$Ba-O(3)^2$	2.795 (3)	Ba–O(4)	2.827 (3)
$Ba-OW^1$	2.832 (5)		
C(1)–O(1)	1.221 (5)	C(1)–O(2)	1.301 (5)
C(1)–C(2)	1.501 (6)	C(2)–C(3)	1.527 (6)
C(2)–C(4)	1.403 (8)	C(3)–O(3)	1.248 (5)
C(3)–O(4)	1.232 (5)	C(4)–C(5)	1.462 (8)

[a] Symmetry operations are given as superscripts: 1 = $x, y, -1 + z$; 2 = ${}^1/_2 + x, {}^1/_2 - y, {}^3/_2 - z$.

Table XIII. Bond Angles (deg) in $Ba(emalH)_2 \cdot H_2O^a$

$O(1)^1-Ba-O(1)$	109.1 (1)	$O(1)^1-Ba-O(1)^3$	65.9 (1)
$O(1)^1-Ba-O(1)^4$	157.7 (1)	$O(1)^1-Ba-O(3)^2$	121.5 (1)
$O(1)^1-Ba-O(3)^5$	66.6 (1)	$O(1)^1-Ba-O(4)$	60.2 (1)
$O(1)^1-Ba-O(4)^4$	101.5 (1)	$O(1)^1-Ba-OW^1$	60.4 (1)
$O(1)-Ba-O(1)^4$	66.7 (1)	$O(1)-Ba-O(3)^2$	127.4 (1)
$O(1)-Ba-O(3)^5$	71.3 (1)	O(1)–Ba–O(4)	60.0 (1)
$O(1)-Ba-O(4)^4$	101.8 (1)	$O(1)-Ba-OW^1$	138.0 (1)
$O(3)^2-Ba-O(3)^5$	115.3 (1)	$O(3)^2-Ba-O(4)$	161.8 (1)
$O(3)^2-Ba-O(4)^4$	82.4 (1)	$O(3)^2-Ba-OW^1$	67.4 (1)
$O(4)-Ba-O(4)^4$	79.7 (2)	$O(4)-Ba-OW^1$	119.9 (1)
O(1)–C(1)–O(2)	122.6 (4)	O(1)–C(1)–C(2)	122.8 (4)
O(2)–C(1)–C(2)	114.5 (4)	C(1)–C(2)–C(3)	110.9 (3)
C(1)–C(2)–C(4)	120.3 (4)	C(3)–C(2)–C(4)	117.6 (4)
C(2)–C(3)–O(3)	116.7 (4)	C(2)–C(3)–O(4)	119.0 (4)
O(3)–C(3)–O(4)	124.2 (4)	C(2)–C(4)–C(5)	122.1 (5)

[a] Symmetry operations as in Table XII, plus the following: 3 = $x, {}^1/_2 - y, -1 + z$; 4 = $x, {}^1/_2 - y, z$; 5 = ${}^1/_2 + x, y, {}^3/_2 - z$.

$[Ba(emalH)_2] \cdot H_2O$. The structure consists of Ba^{2+} cations coordinated to two $emalH^-$ anions and water molecules; as in all previous examples, the units are linked by bridges through the anions and water molecules to form a polymeric aggregate. The barium atom sits on a crystallographic mirror plane, as does the water molecule. The geometry around the barium is shown in Figure 7. The coordination polyhedron at barium is 10-coordinate and consists of four unidentate interactions, two malonate coordination modes, and two coordinated water molecules. The Ba–O distances are in the range 2.795 (3)–2.937 (5) Å, and these and other metrical parameters are normal. Bond lengths and angles are listed in Tables XII and XIII, respectively.

As is shown in Figure 8, each $emalH^-$ ion binds to three different barium ions. The structure can be viewed as consisting of sheets of barium cations that lie on the mirror plane (at $y = {}^1/_4$) and are linked together by $emalH^-$ ions and water molecules.

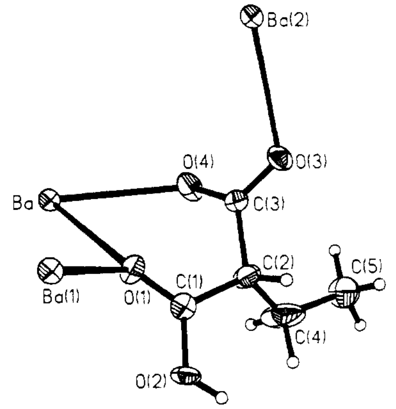

Figure 8. Binding of a single emalH$^-$ ion in $[Ba(emalH)_2]\cdot H_2O$. Atoms labeled Ba(1) and Ba(2) are related to the parent atom by the symmetry operations $x, y, z + 1$; and $x - {}^1/_2, {}^1/_2 - y, 1{}^1/_2 - z$, respectively.

The geometric parameters of the hydrogen ethylmalonate ion agree well with those in the related benzylmalonate ion (vide supra). One of the carboxyl groups [O(1)–C(1)–O(2)] is 7° out of the plane C(1)–C(2)–C(3) while the other forms an angle with the same plane of 57°, and the dihedral angle between carboxyl groups is 63°.

Discussion

The four structures presented here clearly demonstrate that the coordination of Ba^{2+} to Gla and Asa analogues is comparable to that of calcium but in contrast to that observed for the smaller alkaline-earth metals magnesium and beryllium. At present, the limited data available for Be^{2+} and Mg^{2+} suggest that the malonate mode may be the only mode that will be observed for these metals, since in $Be(mal)_2^{2-}$,[28] $Mg(malH)_2\cdot 2H_2O$,[25] and $Mg(Memal)(OH_2)_4$[15] no other mode is observed; there is no obvious a priori reason for this observation, however. For the larger alkaline-earth-metal ions, three coordination modes are possible, and in any given structure one, two, or all three of them might be observed. More significant, however, than the nature of the coordination around any given metal is the overall structure of the complex. For the smaller ions (Be^{2+}, Mg^{2+}), the overall structures are regular and *monomeric*, lacking any interactions between neighboring metal centers. The four barium structures presented here, along with the calcium complexes examined earlier,[15,17,18,23-25] are all *polymeric*, and it has been suggested that the ability of Gla and/or Asa to contribute additional carboxylate groups to these arrays is a major reason for their presence in calcium proteins.[15,17] The present result would suggest that, in principle, barium could bind in much the same way as calcium to such proteins, which would explain the observation that normal prothrombin adsorbs onto barium citrate but that abnormal prothrombin (which lacks the Gla residues) does not.[20-22]

Registry No. $[Ba(bzmalH)_2]\cdot H_2O$ (coordination compound entry), 114595-65-2; $[Ba(bzmal)]\cdot 3H_2O$ (coordination compound entry), 114584-18-8; $[Ba(dmal)]_2\cdot 5H_2O$ (coordination compound entry), 114584-19-9; $[Ba(emalH)_2]\cdot H_2O$ (coordination compound entry), 114584-20-2; $[Ba(bzmalH)_2]\cdot H_2O$ (salt entry), 114584-21-3; $[Ba(bzmal)]\cdot 3H_2O$ (salt entry), 114584-22-4; $[Ba(dmal)]_2\cdot 5H_2O$, 114584-23-5; $[Ba(emalH)_2]\cdot H_2O$, 114584-24-6; prothrombin, 9001-26-7.

Supplementary Material Available: Tables S1–S4, listing hydrogen atom positional parameters, and Tables S5–S8, listing anisotropic thermal parameters (8 pages); Tables S9–S12, listing observed and calculated structure amplitudes (38 pages). Ordering information is given on any current masthead page.

Contribution from the Department of Inorganic Chemistry, The University, Newcastle upon Tyne NE1 7RU, England,
Department of Biochemistry, The University, Liverpool L69 3BX, England, and Department of Molecular Biology,
Research Institute of Scripps Clinic, La Jolla, California 92037

Kinetic Studies on 1:1 Electron-Transfer Reactions Involving Blue Copper Proteins. 16. Reactivity of Plastocyanin from the Green Alga *Scenedesmus obliquus* with Inorganic Redox Partners and Related NMR Studies

Joseph McGinnis,[†] John D. Sinclair-Day,[†] A. Geoffrey Sykes,*[,†] Roy Powls,[‡] Jonathan Moore,[§]
and Peter E. Wright[§]

Received December 10, 1987

The reactivity of plastocyanin from a green algal source, *Scenedesmus obliquus* (estimated PCu^I charge −9 at pH ~7), has been studied for the first time in order to further assess the effect of amino acid sequence variations in naturally occurring plastocyanins. At 25 °C, $I = 0.10$ M (NaCl), and pH <7.5, rate constants with $[Fe(CN)_6]^{3-}$ and $[Co(phen)_3]^{3+}$ as oxidants for PCu^I and with $[Co(phen)_3]^{2+}$ as reductant for PCu^{II} are similar in magnitude to those obtained previously for the higher plant plastocyanins and show similar dependences on pH. Attention is drawn to the possibility that in this and some other instances there may be a small residual reactivity of PCu^I with $[Fe(CN)_6]^{3-}$ at low pH. A novel feature at pH >7.5 is the increase in rate constants giving protein pK_a values of 7.6 ($[Fe(CN)_6]^{3-}$) and 8.2 ($[Co(phen)_3]^{3+}$), confirmed by NMR spectroscopy (pK_a = 7.8) as a deprotonation/protonation of His59, a residue not present in the higher plant plastocyanins. Also from NMR measurements a sensitivity to active-site protonation at His59 and to His59 protonation at the active site is indicated, although there is no direct link between the two and the imidazole ring of His59 is 10–12 Å from the Cu site. There is however no evidence for electron transfer from the 59–61 binding site. At pH 7.56 no saturation kinetic behavior is observed with $[Co(phen)_3]^{3+}$ ($K < 25$ M^{-1}), which is attributable to the lower (−3 instead of −4) charge at residues 42–45, but at pH 9.1, when His59 is acid dissociated, such behavior is observed ($K = 50$–100 M^{-1}). From ^{1}H NMR line-broadening experiments at pH 6.3 and 7.0 using Cr(III) analogue complexes, it has been demonstrated that $[Cr(CN)_6]^{3-}$ produces almost no specific broadening effects. With $[Cr(phen)_3]^{3+}$ binding to *S. obliquus* PCu^I is observed over a delocalized region of the protein surface including the negatively charged residues 42–44 and 60–61. Deletions at positions 57 and 58 in the aligned sequences bring these two regions sufficiently close together for reaction at the 42–44 site to be affected by the state of protonation of His59.

Introduction

Plastocyanin is a single blue (type 1) copper metalloprotein involved in electron transport ($E° = 370$ mV at pH 7) between photosystems II and I of the chloroplasts in higher plants and algae.[1] Normally it consists of a single polypeptide chain of ca. 99 amino acids (mol wt 10 500). Plastocyanins from 15 higher plants, 3 green algae, and 1 blue-green alga have been fully sequenced. [The fully sequenced plastocyanins are as follows:

[†] The University, Newcastle upon Tyne.

[‡] The University, Liverpool.

[§] Research Institute of Scripps Clinic.

[1] Sykes, A. G. *Chem. Soc. Rev.* **1985**, 283.

0020-1669/88/1327-2306$01.50/0